INTERNATIONAL JOURNAL FOR NUMERICAL METHODS IN FLUIDS
Int. J. Numer. Meth. Fluids 2001; **36**: 639–657 (DOI: 10.1002/fld.149)

A convergence study of two ocean models applied to a density driven flow

Helge Avlesen[a,*,1], Jarle Berntsen[b] and Terje O. Espelid[a]

[a] *Department of Informatics, University of Bergen, Thormøhlensgt., Bergen, Norway*
[b] *Department of Mathematics, University of Bergen, Johs. Bruns gt., Bergen, Norway*

SUMMARY

A three-dimensional, baroclinic and rotational benchmark for hydrostatic coastal ocean models is suggested. The computational domain is a quadratic basin 200×200 km horizontally and 200 m deep. The lateral boundaries are closed. Solutions to the problems are estimated with two different sigma co-ordinate models, both for the diagnostic and the prognostic case. Grid- and time-converged results are presented. For the transports, convergence within two significant digits is reported. Copyright © 2001 John Wiley & Sons, Ltd.

KEY WORDS: baroclinic benchmark; convergence study; model intercomparison; ocean model; test case

1. BACKGROUND

Numerical regional scale ocean models are frequently used both in research and management of the environment and ocean resources. Methods for quantitative assessment of three-dimensional ocean model skills are still in their infancy, and qualitative assessment of model outputs is common in the development of numerical ocean models. One exception seems to be the assessment of tidal model skills, see Reference [1].

Several attempts have been made to develop methods for quality assessment of residual model outputs from three-dimensional baroclinic coastal ocean models, e.g. comparison of observations and model outputs. Examples are found in References [2,3]. Such attempts are however difficult because what we often have is point observations whereas the model outputs represent averages in both time and space. There is also a general lack of observations. In comparison between observations and model outputs, it is also the quality of the whole model system including the bathymetry, the initial fields, the boundary values and the forcing fields that are assessed.

* Correspondence to: Department of Informatics, University of Bergen, Thormøhlensgt. 55, 5020 Bergen, Norway. Tel.: +47 55 584035; fax: +47 55 584199.
[1] E-mail: avle@ii.uib.no

Received November 1998
Revised June 1999

For industrial fluid flow problems the establishment of a series of benchmarks has proved to be very useful in the quality assessment of numerical codes [4]. To have at least a few agreed upon solutions is of great value both in the development of new codes, and under the modification of an existing code.

For prognostic ocean flow problems involving stratification, based on the full three-dimensional equations normally used in ocean models, it is impossible to produce an analytical solution. The one exception is the trivial solution, which we have only for cases with no initial flow and no forcing.

At the symposium on assessment of coastal ocean model skills [5], several benchmarks with corresponding solutions from five ocean models were presented [2]. The solutions differed too much to be useful for more than a qualitative assessment. Even if the problems were simplified compared to real world problems, they were apparently still too difficult for the codes to produce a common solution. Another problem was that the subgrid scale parameterizations to be used were not specified, and therefore the problems were not closed mathematically.

At the Ocean Modelling and Remote Sensing Laboratory at Rutgers University, a variety of idealized test problems have been devised for evaluation of three-dimensional ocean circulation models, however to our knowledge convergence in time and space to a solution produced with more than one model is not yet demonstrated. One reason is probably that even if the cases are idealized they are not trivial. Some of these problems are described in a recent book by Haidvogel and Beckmann [6].

Over the last few years we have tried to establish converged solutions for problems involving combinations of stratification, Coriolis effects, open boundary forcing, topographic effects and wind forcing. We have however found this to be much more difficult than expected, and understand that model outputs may vary as much as demonstrated in the MOMOP exercise for instance.

In this paper we try to establish a converged solution for a test problem complex enough to measure fundamental qualities of numerical schemes in ocean models, but otherwise as simple as possible.

Such a solution should be well suited as a checkpoint in code development.

We want such a benchmark to feature at least the following properties:

- A simple set up.
- Stringent specification.
- Three-dimensional effects from non-linearities, stratification and rotation, and a fully prognostic solution in time.
- Converged solutions from more than one model.

As a starting point we propose a simple three-dimensional, hydrostatic and baroclinic test case, including effects of rotation, non-linearities, and a transport equation for density. The depth is constant, and the computational domain is closed, density gradients in the beginning are small, and the viscosities are chosen to be large and constant in both time and space.

We present a converged solution obtained by two ocean models that both apply the Arakawa C-grid and the sigma co-ordinate system. Solutions for both the diagnostic case and prognostic case are given. When implementing ocean models for new problems it is common

practice to run the model in diagnostic mode first[2], using a fixed density. A diagnostic solution of a test problem is therefore of interest to check that the model approximates the equations of continuity and momentum in a satisfactory way. The next natural step would be to check that the prognostic solution is also in agreement with a converged reference solution. The reference solution will of course be the solution obtained on the finest mesh with the shortest time step.

One benchmark cannot answer all challenges of ocean modelling, so to get an overall impression of the performance and accuracy of the numerical engine we will need additional converged benchmarks each approaching other problematic areas such as turbulence, bathymetry, irregular boundaries, open boundary conditions, resolution of fronts, etc.

2. THE MODEL PROBLEM

The prognostic variables describing our problem are the three velocity components U, V and W, the pressure P and the density ρ. Using the Boussinesq approximation and the hydrostatic approximation, we can write the standard momentum equations in Cartesian co-ordinates as

$$\frac{\partial U}{\partial x}+\frac{\partial V}{\partial y}+\frac{\partial W}{\partial z}=0 \tag{1}$$

$$\frac{\partial U}{\partial t}+\vec{U}\cdot\nabla U+W\frac{\partial U}{\partial z}-fV=-\frac{1}{\rho_0}\frac{\partial P}{\partial x}+\frac{\partial}{\partial z}\left(K_M\frac{\partial U}{\partial z}\right)+F_U \tag{2}$$

$$\frac{\partial V}{\partial t}+\vec{U}\cdot\nabla V+W\frac{\partial V}{\partial z}+fU=-\frac{1}{\rho_0}\frac{\partial P}{\partial y}+\frac{\partial}{\partial z}\left(K_M\frac{\partial V}{\partial z}\right)+F_V \tag{3}$$

$$P=g\rho_0\eta+g\int_z^0\rho(s)\,\mathrm{d}s \tag{4}$$

$$\frac{\partial \rho}{\partial t}+\vec{U}\cdot\nabla\rho+W\frac{\partial \rho}{\partial z}=\frac{\partial}{\partial z}\left(K_H\frac{\partial \rho}{\partial z}\right)+F_\rho \tag{5}$$

where η is the surface elevation with respect to the zero level. The z-axis is positive upward, with the origin at the resting sea surface. The horizontal diffusion terms are all written in the form

$$F_\phi=\frac{\partial}{\partial x}\left(A\frac{\partial \phi}{\partial x}\right)+\frac{\partial}{\partial y}\left(A\frac{\partial \phi}{\partial y}\right) \tag{6}$$

[2] This may not be a correct use of the word 'diagnostic' since some of the quantities are evolving, but it is commonly used to describe this type of run.

We take the following parameters to be constant:

Coriolis parameter: $f = 1.3 \times 10^{-4}\ \mathrm{s}^{-1}$
Reference density: $\rho_0 = 1025.0\ \mathrm{kg\ m}^{-3}$
Effective vertical viscosity and diffusivity: $K_M = K_H = 0.01\ \mathrm{m}^2\ \mathrm{s}^{-1}$
Effective horizontal viscosity and diffusivity: $A_M = A_H = 10000\ \mathrm{m}^2\ \mathrm{s}^{-1}$
Acceleration due to gravity: $g = 9.806\ \mathrm{m\ s}^{-2}$

The subscript M refers to the momentum equations, and the subscript H to the equation for density.

After transformation to the sigma co-ordinate system, details given in Blumberg and Mellor [7], we can rewrite the equation system as

$$\frac{\partial UD}{\partial x} + \frac{\partial VD}{\partial y} + \frac{\partial \omega}{\partial \sigma} + \frac{\partial \eta}{\partial t} = 0 \tag{7}$$

$$\frac{\partial UD}{\partial t} + \frac{\partial U^2 D}{\partial x} + \frac{\partial UVD}{\partial y} + \frac{\partial U\omega}{\partial \sigma} - fVD + gD\frac{\partial \eta}{\partial x} = \frac{\partial}{\partial \sigma}\left(\frac{K_M}{D}\frac{\partial U}{\partial \sigma}\right) - \frac{gD^2}{\rho_0}\int_\sigma^0 \frac{\partial \rho}{\partial x}\,\mathrm{d}\sigma + DF_U \tag{8}$$

$$\frac{\partial VD}{\partial t} + \frac{\partial UVD}{\partial x} + \frac{\partial V^2 D}{\partial y} + \frac{\partial V\omega}{\partial \sigma} + fUD + gD\frac{\partial \eta}{\partial y} = \frac{\partial}{\partial \sigma}\left(\frac{K_M}{D}\frac{\partial V}{\partial \sigma}\right) - \frac{gD^2}{\rho_0}\int_\sigma^0 \frac{\partial \rho}{\partial y}\,\mathrm{d}\sigma + DF_V \tag{9}$$

$$DF_\phi = \frac{\partial}{\partial x}\left(DA_M\frac{\partial \phi}{\partial x}\right) + \frac{\partial}{\partial y}\left(DA_M\frac{\partial \phi}{\partial y}\right)$$

$$\frac{\partial \rho D}{\partial t} + \frac{\partial \rho UD}{\partial x} + \frac{\partial \rho VD}{\partial y} + \frac{\partial \rho \omega}{\partial \sigma} = \frac{\partial}{\partial \sigma}\left(\frac{K_H}{D}\frac{\partial \rho}{\partial \sigma}\right) + DF_\rho, \tag{10}$$

$$DF_\rho = \frac{\partial}{\partial x}\left(DA_H\frac{\partial \rho}{\partial x}\right) + \frac{\partial}{\partial y}\left(DA_H\frac{\partial \rho}{\partial y}\right)$$

The independent variables (x, y, z, t) are transformed to (x^*, y^*, σ, t^*) where

$$x^* = x, \quad y^* = y, \quad \sigma = \frac{z - \eta}{H + \eta}, \quad t^* = t \tag{11}$$

We have introduced the static depth H, which is the depth when the ocean is at rest, and the total (dynamical) depth $D = H + \eta$. The vertical velocity ω of this system is defined as

$$\omega \equiv W - U\left(\sigma\frac{\partial D}{\partial x} + \frac{\partial \eta}{\partial x}\right) - V\left(\sigma\frac{\partial D}{\partial y} + \frac{\partial \eta}{\partial y}\right) - \left(\sigma\frac{\partial D}{\partial t} + \frac{\partial \eta}{\partial t}\right) \tag{12}$$

To make comparison with other models not using the sigma co-ordinate system easier, a number of terms from the co-ordinate transformation are left out. In this study $\partial H/\partial x_i = 0$, so the effect of the terms related to bathymetry should be negligible. The terms related to elevation are also generally assumed to be small, this may not be the case during the initial transient phase.

We consequently use x, y and t in our notation since these are unchanged during the transformation.

2.1. Geometry and boundary conditions

The model domain is the quadratic basin $0 \le x \le L_x$, $0 \le y \le L_y$. $L_x = L_y = 200000$ m, with vertical walls on all sides. The depth H is given as $H(x, y) = 200$ m for all x and y. At the bottom we have $U = V = 0$, no flux and full slip conditions on the lateral boundaries. At the free surface we have zero wind stress

$$K_M \frac{\partial \vec{U}}{\partial z} = 0, \quad z = \eta \tag{13}$$

The bottom stress is given by the quadratic law

$$K_M \frac{\partial \vec{U}}{\partial z} = c_d (U_b^2 + V_b^2)^{1/2} \vec{U}_b, \quad z = H(x, y) \tag{14}$$

where

$$c_d = \max\left[0.0025, \frac{\kappa^2}{(\ln(z_b/z_0))^2}\right] \tag{15}$$

Subscript 'b' denotes variables evaluated in the grid point nearest to the bottom. The Von Karman constant $\kappa = 0.4$ and the bottom roughness length $z_0 = 0.01$ m. These settings are taken from Blumberg and Mellor [7].

2.2. Initial values

To describe the initial density field, we define the two metrics

$$r_h = \sqrt{(x - 100000)^2 + (y - 100000)^2} \tag{16}$$

$$r_v = 1000z \tag{17}$$

The density at $t = 0$ is then given by the expressions

$$\rho_h(x, y) = \rho_c - \Delta\rho \tanh(r_h/\Delta r) \tag{18}$$

$$\rho(x, y, z) = \rho_h(x, y)(1 - \tanh(r_v/\Delta r)) + \rho_0 \tanh(r_v/\Delta r) \tag{19}$$

where $\rho_c = 1024$ kg m^{-3}, $\Delta\rho = 4$ kg m^{-3}, $\Delta r = \sqrt{3} \times 50\,000$ m. At the surface this means a circular core of density 1024 kg m^{-3} decreasing outward towards the boundaries to 1020 kg m^{-3}. As we move towards the bottom this distribution gradually change towards the reference density $\rho_0 = 1025$ kg m^{-3}.

Initially U and V are derived from the thermal wind relations

$$f\frac{\partial U}{\partial z} = \frac{g}{\rho_0}\frac{\partial \rho}{\partial y} \tag{20}$$

$$f\frac{\partial V}{\partial z} = -\frac{g}{\rho_0}\frac{\partial \rho}{\partial x} \tag{21}$$

The vertical velocity W is initially equal to 0. The initial free surface is determined from

$$\frac{\partial \tilde{\eta}}{\partial x} = \frac{1}{\rho_0}\int_{-H}^{0}\frac{\partial \rho}{\partial x}\,\mathrm{d}z \tag{22}$$

$$\frac{\partial \tilde{\eta}}{\partial y} = \frac{1}{\rho_0}\int_{-H}^{0}\frac{\partial \rho}{\partial y}\,\mathrm{d}z \tag{23}$$

assuming $\hat{\eta}(0, 0) = 0$ m. The average $\hat{\eta}$ is then computed from

$$\hat{\eta} = \frac{1}{L_x \times L_y}\int_0^{L_x}\int_0^{L_y}\tilde{\eta}\,\mathrm{d}x\,\mathrm{d}y \tag{24}$$

The initial velocity and density field are shown in Figure 1, where we also have introduced $\sigma_t = \rho - 1000$ kg m^{-3}. Finally, an initial surface which averaged over the basin will be zero is computed from $\eta = \tilde{\eta} - \hat{\eta}$.

3. NUMERICAL METHODS

The numerical results presented in this work were obtained from the two ocean models we will refer to as POM (the Princeton Ocean Model) and BOM (the Bergen Ocean Model). Detailed information for POM can be found in Reference [7] and for BOM in Reference [8].

Both models are sigma co-ordinate ocean models, and also use the same spatial grid, the so called Arakawa C-grid [9]. The main differences between the two models are the time stepping scheme, the advection scheme and the method for estimating the surface elevation.

3.1. The Princeton ocean model

POM uses a mode splitting approach. The idea is to propagate the full depth integrated momentum equations in time with the leapfrog scheme, using short time steps corresponding to the CFL criterion for the external mode. This gives the elevation as output, which is then

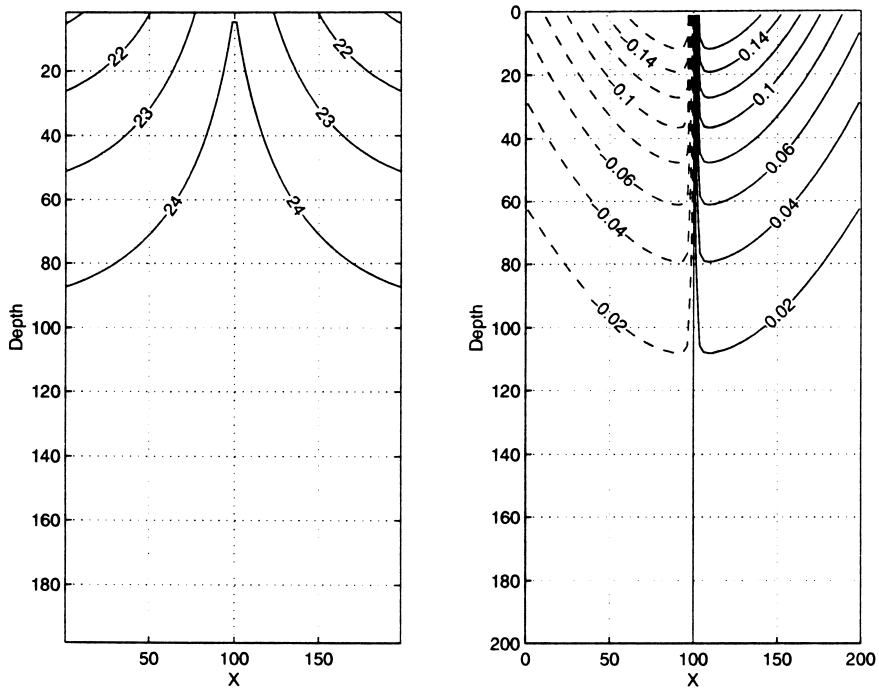

Figure 1. Initial density σ_t (left) and initial velocity (right) V (m s^{-1}) for $y = L_y/2$. Horizontal units are in km, vertical units are in metres.

used in the full three-dimensional equations and propagated with a time step that can be a factor 20–30 times larger. The leapfrog strategy is used consequently, also for advection. We chose to march forward with an external time step one fourth of the internal mode time step.

The version of the Princeton Ocean Model used is written in standard, single precision Fortran 77, and can presently be found at:
http://www.aos.princeton.edu/WWWPUBLIC/htdocs.pom/pom97.f

A discussion on the form of the equations used in POM can be found in Reference [10]. To solve our model equations we did a few simple modifications in POM described in the Appendix.

3.2. A short description of the explicit BOM

In the version of BOM applied a forward-backward type method is used to propagate the momentum equations in time. The main idea is to do a forward Euler step on the full three-dimensional momentum equations to predict the velocity, then a backward step on the equation of continuity to find the elevation. The order of the calculation of the momentum equations are switched each time step. The advection terms are approximated using a

Lax–Wendroff discretization in time. Note that this version of BOM has no mode splitting, and since all terms are propagated explicitly in time, the time step must obey the CFL criterion related to the surface gravity waves. A more detailed description of the time stepping used in the explicit version of BOM can be found in Reference [11].

We chose to run POM with an internal mode time step four times as large as the external mode. POM is therefore approximating the elevation more accurately for the longest time steps of the simulations.

3.3. Meshes

The simulations were run on a series of meshes labeled A–D, with the number of ocean cells ranging from 900 to 345600. Details for each mesh are given in Table I. The vertical grid was generated manually. The general idea is that we start with a constant spacing from $\sigma = 0$ to $\sigma = -0.3$, then $\Delta\sigma$ increase linearly to $\sigma = -0.9$ or -0.95, and then finally we place a couple of points near the bottom. The idea is of course to resolve the surface and bottom gradients as good as possible by using some extra grid points.

4. RESULTS

Two series of simulations were done, a diagnostic run with the initial density field held constant in time, and one fully prognostic. Both series of simulations were run for 10 days with up to five different three-dimensional time steps, and on four meshes. Normally, to obtain realistic physics, horizontal viscosity and diffusivity vary with the resolution, but as we want to evaluate the numerics of the model we use the same constant values for all grids. The horizontal diffusivity is very 'unphysical', but this is just an effective remedy to make something happen in finite time on a modest computer.

We expected the diagnostic run to reach a steady state solution, and that the two models converged toward the same answer. The prognostic solution should show an exponentially damped development in time.

4.1. Model outputs

In order to illustrate the convergence and accuracy of the two models, we have chosen to focus on the time-series for the following quantities:

1. A kinetic energy norm, given by the expression

Table I. The grids.

Mesh	A	B	C	D
Horizontal grid size	20 km	10 km	5 km	2.5 km
Number of cells	900 ($10\times10\times9$)	6000 ($20\times20\times15$)	44 800 ($40\times40\times28$)	345 600 ($80\times80\times54$)

$$\frac{1}{2\mathrm{VOL}}\int_0^{L_x}\int_0^{L_y}\int_{-H}^{\eta}\rho(U^2+V^2+W^2)\,\mathrm{d}x\,\mathrm{d}y\,\mathrm{d}z,$$

$$\mathrm{VOL}=\int_0^{L_x}\int_0^{L_y}(\eta(x,y,t)+H(x,y))\,\mathrm{d}x\,\mathrm{d}y$$

All integrals are evaluated with a second-order accurate scheme.

2. The net transport through a section from $(x, y) = (L_x/2, L_y/2)$ to $(L_x, L_y/2)$.
3. The velocity component V in $(X = 3/4L_x, Y = 1/2L_y, \sigma = -0.2)$, obtained by linear interpolation from the various meshes.

This is inspired by the hierarchical approach used by Røed *et al.* [2], and we believe that these time-series should be fairly easy to extract from any model for comparison.

4.2. The diagnostic run

Tables II and III demonstrate that we for all measured quantities, after a simulation over 10 days, have two digits convergence in space for both POM and BOM, four digits convergence in time for BOM, and finally five digits convergence in time for POM. The time step given for POM is the time step for the three-dimensional part of the code.

The numbers also show that BOM converges toward a lower level for the measured quantities than those for POM, indicating that BOM looses energy faster. For the time stepping scheme, BOM uses a first-order forward–backward Euler type scheme, which is known to be more diffusive in time than the filtered leapfrog approach of POM. As both

Table II. Results for the diagnostic run with BOM after 240 h.

Time step (s)	A	B	C	D
Transport				
240	0.588807E+05			
120	0.588356E+05	0.602765E+05		
60	0.588427E+05	0.602315E+05	0.657977E+05	
30	0.588173E+05	0.602010E+05	0.657846E+05	0.659234E+05
15	0.588198E+05	0.603063E+05	0.657221E+05	0.659254E+05
Kinetic energy norm				
240	0.491310E−03			
120	0.491576E−03	0.462519E−03		
60	0.491712E−03	0.462652E−03	0.455114E−03	
30	0.491778E−03	0.462717E−03	0.455181E−03	0.452986E−03
15	0.491815E−03	0.462765E−03	0.455203E−03	0.453022E−03
Velocity in $(X, Y, Z) = (3/4L_x, 1/2L_y, -40\ \mathrm{m})$ $(\sigma = -0.2)$				
240	0.427133E−01			
120	0.427071E−01	0.397627E−01		
60	0.427059E−01	0.397554E−01	0.393141E−01	
30	0.427035E−01	0.397510E−01	0.393106E−01	0.391197E−01
15	0.427029E−01	0.397555E−01	0.393063E−01	0.391181E−01

Table III. Results for the diagnostic run with POM after 240 h.

Time step (s)	A	B	C	D
Transport				
240	0.612812E+05	0.626722E+05		
120	0.612910E+05	0.626818E+05	0.684252E+05	
60	0.612971E+05	0.626851E+05	0.684286E+05	0.685884E+05
30	0.612993E+05	0.626868E+05	0.684310E+05	0.685900E+05*
15	0.612995E+05	0.626875E+05	0.684324E+05	0.685911E+05
Kinetic energy norm				
240	0.516641E−03	0.486124E−03		
120	0.516643E−03	0.486126E−03	0.478230E−03	
60	0.516644E−03	0.486127E−03	0.478231E−03	0.475737E−03
30	0.516644E−03	0.486128E−03	0.478232E−03	0.475737E−03*
15	0.516643E−03	0.486128E−03	0.478232E−03	0.475737E−03
Velocity in $(X, Y, Z) = (3/4L_x, 1/2L_y, -40\,m)$ $(\sigma = -0.2)$				
240	0.438242E−01	0.407967E−01		
120	0.438248E−01	0.407972E−01	0.403473E−01	
60	0.438251E−01	0.407974E−01	0.403476E−01	0.401535E−01
30	0.438252E−01	0.407976E−01	0.403477E−01	0.401535E−01*
15	0.438253E−01	0.407976E−01	0.403478E−01	0.401536E−01

* Indicates increased smoothing.

methods use second-order schemes for the advection of momentum, Lax–Wendroff (BOM) and leapfrog (POM), it is therefore likely that the time stepping of the surface gravity waves is the main cause of the slightly lower energy level of BOM.

We also observe that as we refine the mesh we get a higher decrease of energy in time. We believe the reason for this is that the increased resolution made the models predict a larger bottom velocity gradient. The time series in Figures 2 and 3 show the expected development of the flow into a steady state solution. We observe that the solution oscillates in time, we identify a fast mode with a period around 1 h and a slower mode with a period of approximately 15 h. We expect the fast mode to be related to surface gravity waves. A simple one-dimensional analysis gives periods for the first three modes to be 2.5, 1.254 and 0.836 h.

The slow oscillation with period around 15 h is likely to be an effect of the constant baroclinic forcing. We believe the observed oscillation to be the numerical scheme trying to adjust itself around an equilibrium state dictated by the constant density field, and therefore shows oscillations of the same frequency as a horizontal sloshing of the density field would give. If we use the formula $\sqrt{g'H} = \sqrt{\Delta\rho/\rho gH}$ to approximate the horizontal speed of the adjustment oscillation of the solution, and further assume the horizontal density difference $\Delta\rho$ to be of order 3–5 $\mathrm{kg\,m^{-3}}$, we find this speed to be in the interval [2.4, 3.3] $\mathrm{m\,s^{-1}}$. The horizontal length-scale of our sea is 200 km so disturbances with a speed in this interval would use between 16.8 and 23.1 h from the centre to the wall and back.

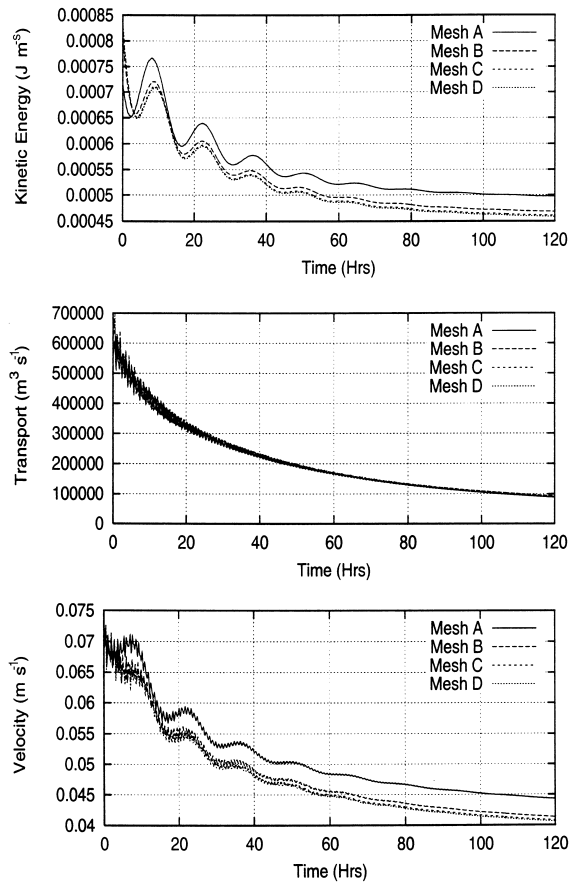

Figure 2. Time-series of the diagnostic BOM, $dt = 15$.

Figure 4 shows how the constant driving density field sets up a strong counter-clockwise eddy near the surface, and a clockwise eddy near the bottom, giving a downwelling effect. We observe that the eddy near the bottom increases in both strength and scale as we propagate the solution in time.

4.3. The prognostic run

In this section we present results from the fully prognostic runs. Tables IV and V show that for POM and BOM we have obtained two digits convergence both in time and space. We also observe that POM and BOM predict the velocity in our chosen location, after a 10-day long simulation, with three digits agreement. In Figures 5 and 6 we observe the expected exponential decrease in the measured quantities. We can also identify oscillations of period ≈ 1 h due

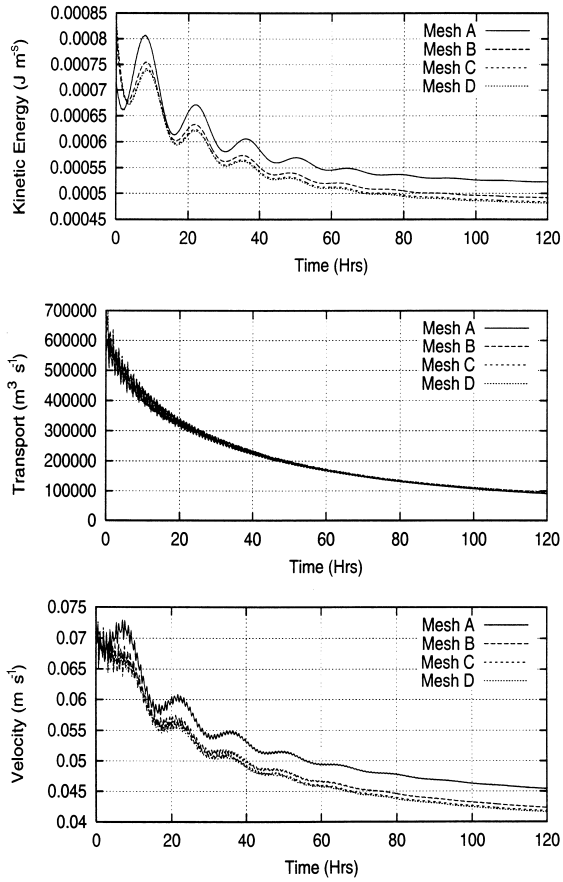

Figure 3. Time-series of the diagnostic POM, $dt = 15$.

to the fast surface gravity waves, and very weak oscillations of period 15 h. Figure 7 shows the expected development of the velocity component V at $y = L_y/2$. Small velocities near the bottom due to friction, very small effects of friction near lateral boundaries, and the field loose vertical structure as the time passes, and the density is fully horizontally mixed (see Figure 8).

4.4. Limitations

A well known weak point with the Arakawa C-grid is the necessary approximation of U in V points and vice versa. We have chosen a linear interpolation for this, and hence introduce an interpolation error of second-order.

Both models apply the sigma co-ordinate system in the vertical, and this introduces extra terms in the full equations, which we have chosen to neglect. For our flat bottom case these terms should have a small or no effect.

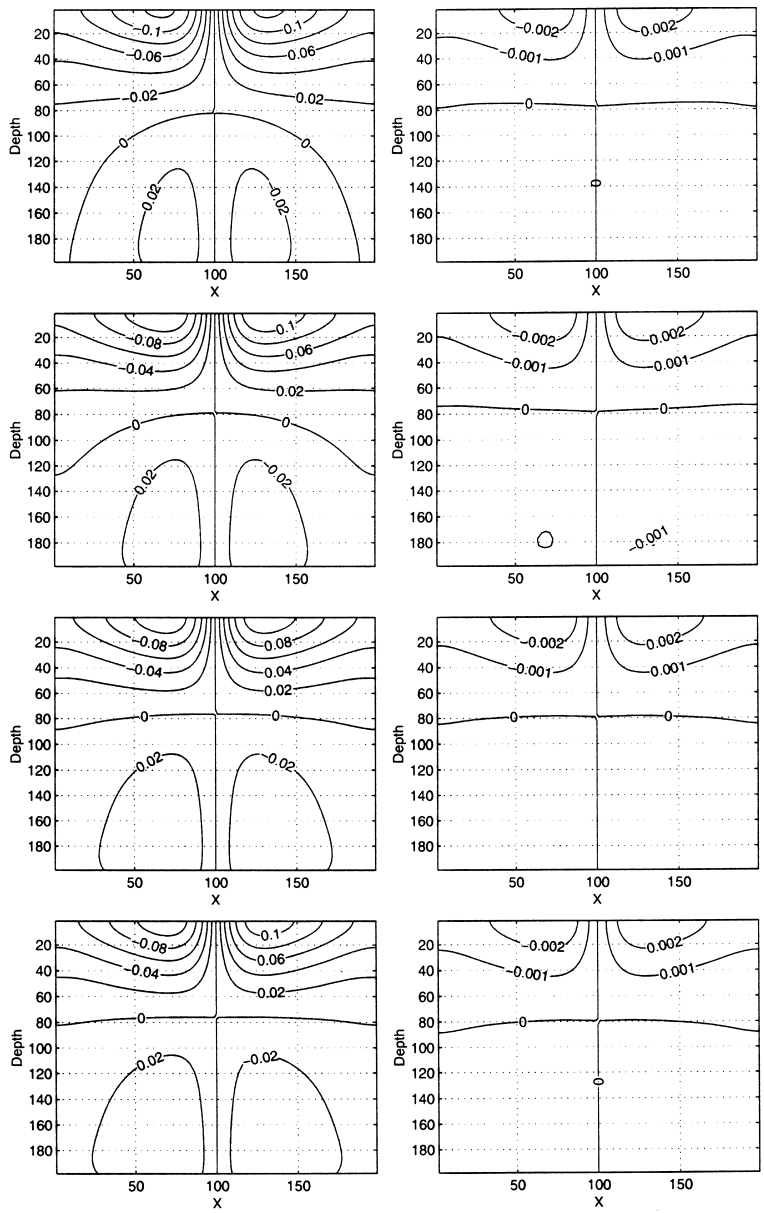

Figure 4. Diagnostic run: velocity $V(x, z)$ for $y = L_y/2$. BOM (left) and the difference $V_{\mathrm{POM}} - V_{\mathrm{BOM}}$ (right) after 1, 2, 5 and 10 days. Horizontal units are in km, vertical units in metres.

Table IV. Results for the prognostic run with POM after 240 h.

Time step (s)	A	B	C	D
Transport				
240	0.618055E+04	0.605921E+04		
120	0.619588E+04	0.607441E+04	0.599881E+04	
60	0.620527E+04	0.608100E+04	0.600562E+04	0.599777E+04
30	0.620970E+04	0.608412E+04	0.600916E+04	0.600050E+04*
15	0.621174E+04	0.608595E+04	0.601121E+04	0.600337E+04
Kinetic energy norm				
240	0.596424E−07	0.576987E−07		
120	0.600162E−07	0.580367E−07	0.566779E−07	
60	0.602108E−07	0.582106E−07	0.568516E−07	0.566862E−07
30	0.603085E−07	0.582964E−07	0.569400E−07	0.567696E−07*
15	0.603600E−07	0.583474E−07	0.569899E−07	0.568246E−07
Velocity in $(X, Y, Z) = (3/4L_x, 1/2L_y, -40\text{ m})$ $(\sigma = -0.2)$				
240	0.347990E−03	0.339993E−03		
120	0.349095E−03	0.341052E−03	0.337709E−03	
60	0.349850E−03	0.341603E−03	0.338247E−03	0.338036E−03
30	0.350121E−03	0.341712E−03	0.338328E−03	0.338083E−03*
15	0.350667E−03	0.342338E−03	0.338696E−03	0.339045E−03

* Indicates increased smoothing.

Table V. Results for the prognostic run with BOM after 240 h.

Time step (s)	A	B	C	D
Transport				
240	0.618627E+04			
120	0.618562E+04	0.607086E+04		
60	0.620094E+04	0.607084E+04	0.599923E+04	
30	0.620986E+04	0.607120E+04	0.600312E+04	0.599285E+04
15	0.620256E+04	0.607369E+04	0.600142E+04	0.598745E+04
Kinetic energy norm				
240	0.598842E−07			
120	0.599265E−07	0.580594E−07		
60	0.601572E−07	0.580716E−07	0.567578E−07	
30	0.603126E−07	0.580991E−07	0.568322E−07	0.566529E−07
15	0.601795E−07	0.581519E−07	0.567988E−07	0.565611E−07
Velocity in$(X, Y, Z) = (3/4L_x, 1/2L_y, -40\text{ m})$ $(\sigma = -0.2)$				
240	0.348680E−03			
120	0.348455E−03	0.341110E−03		
60	0.349753E−03	0.341135E−03	0.338058E−03	
30	0.350160E−03	0.341214E−03	0.338422E−03	0.336934E−03
15	0.350816E−03	0.341923E−03	0.338890E−03	0.339348E−03

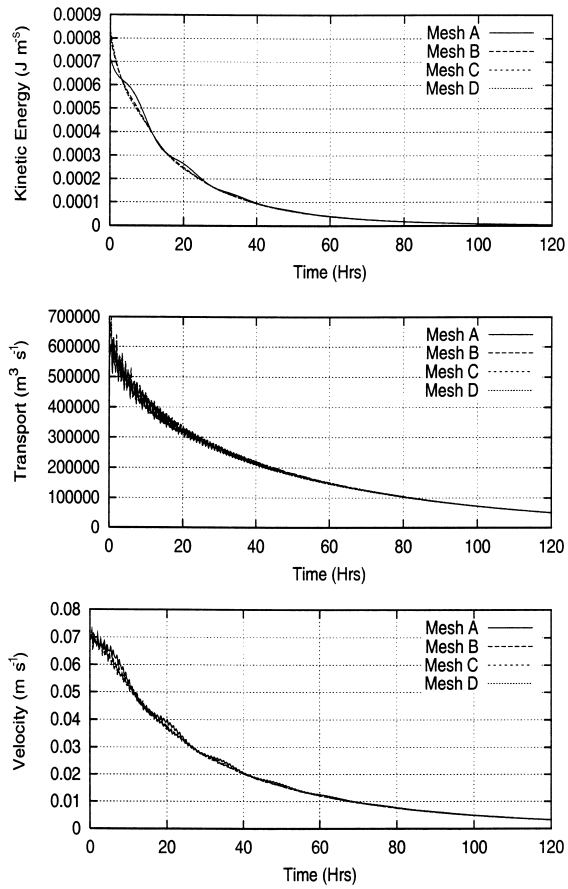

Figure 5. Time-series of the prognostic BOM, $dt = 15$.

On the second finest time step on mesh D using POM, it was necessary to increase the smoothing parameter of the asselin filter to get a stable run. The parameter SMOTH usually was 0.05, the entries marked * were found with SMOTH = 0.4. The reason for this instability is not clear, possibly a computational mode.

5. CONCLUSIONS

We have proposed a prognostic, three-dimensional baroclinic test case for numerical ocean models. The domain is a closed quadratic basin with a flat bottom, with no wind forcing. The

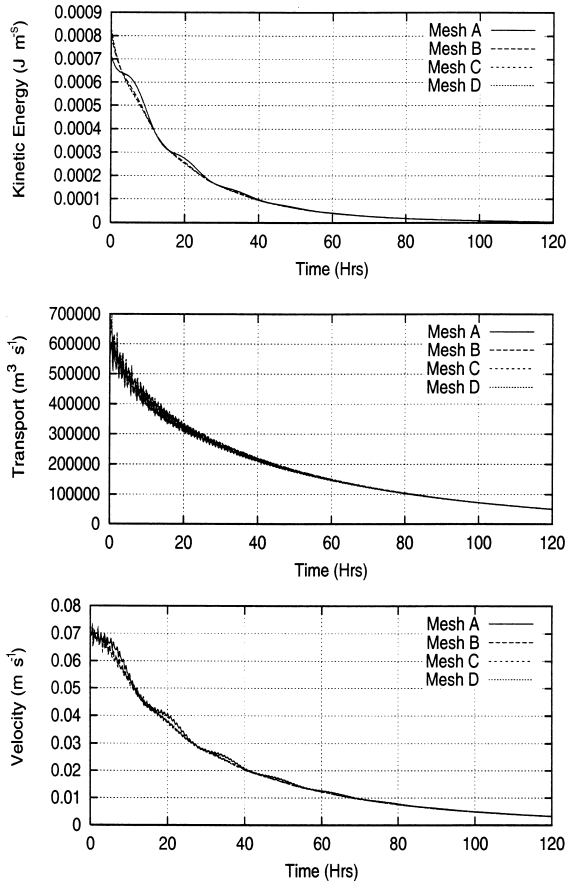

Figure 6. Time-series of the prognostic POM, $dt = 15$.

system is released from an initial geostrophic balance, with a symmetric density distribution with light water along the boundaries.

The test case is meant to focus on the accuracy and convergence of the basic numerical engine of a numerical ocean model, in particular three-dimensional effects of rotation and the density field. The geometry is chosen because of its simplicity, and the initial conditions should give a good indication on the quality of the response to a realistic shelf problem.

We have also presented grid-converged results within two digits, obtained with two sigma co-ordinate ocean models.

Despite the case being simplistic it has already been used to reveal and correct weaknesses in the numerical schemes of both models. The two models did not converge to the presented solutions before they were altered. In our opinion this test case would therefore be useful to test other ocean models.

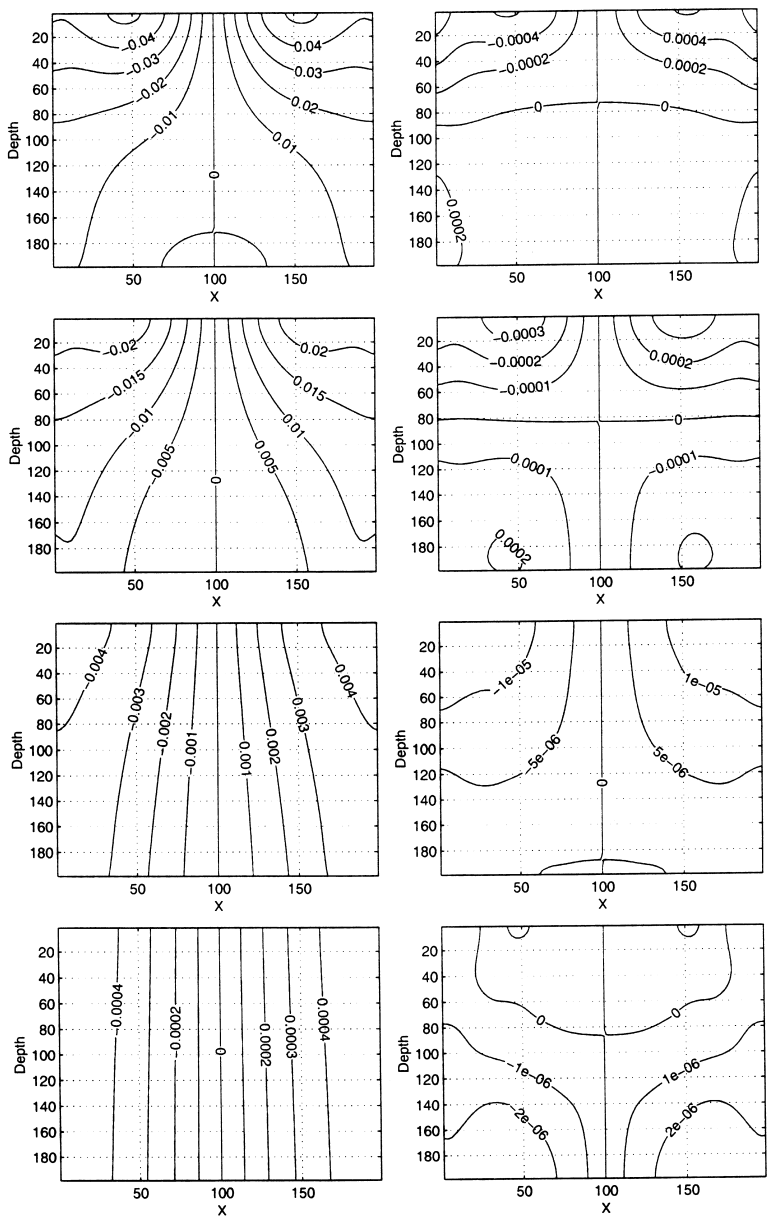

Figure 7. Prognostic run: velocity $V(x, z)$ for $y = L_y/2$. BOM (left) and the difference $V_{\mathrm{POM}} - V_{\mathrm{BOM}}$ (right) after 1, 2, 5 and 10 days. Horizontal units are in km, vertical units are in metres.

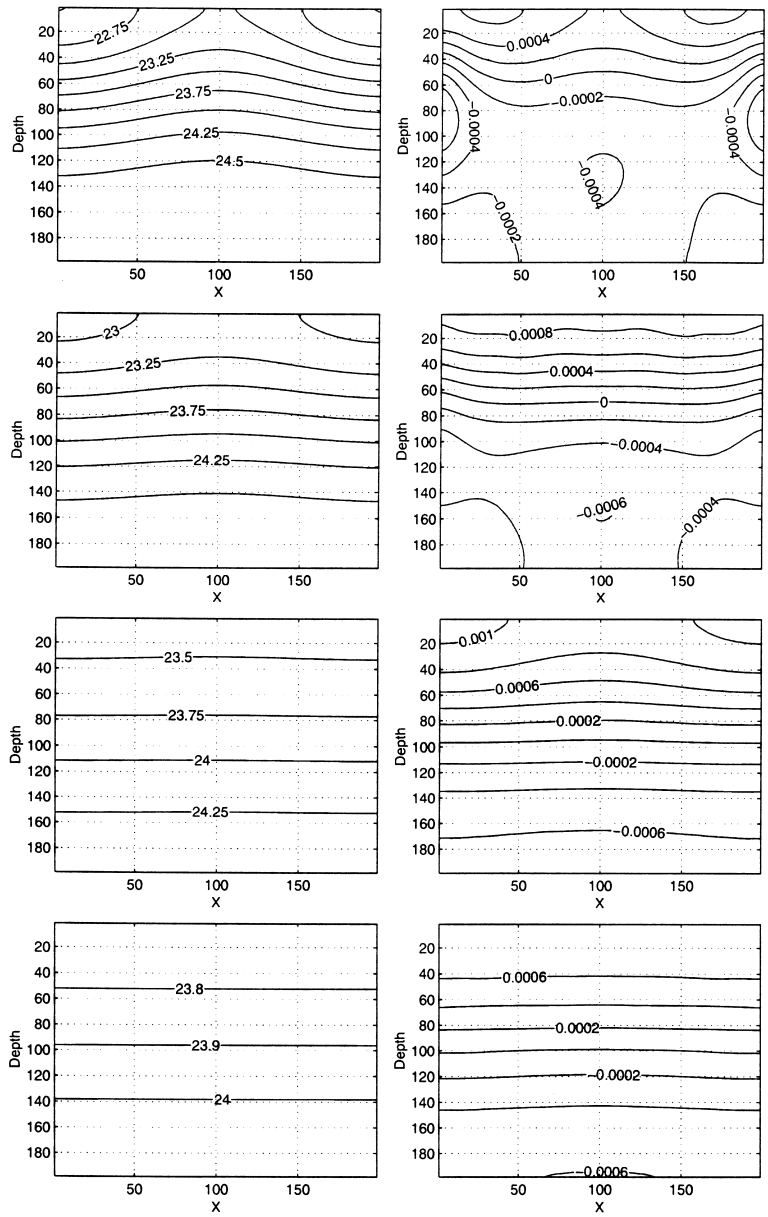

Figure 8. Density σ_t in $y = L_y/2$ for BOM (left) and the difference $\sigma_{t-\mathrm{POM}} - \sigma_{t-\mathrm{BOM}}$ (right) after 1, 2, 5 and 10 days. Horizontal units are in km, vertical units are in metres.

APPENDIX A. MODIFICATIONS TO `pom97.f`

To solve our model equations we modified the following routines of the code:

- main program: solve for density instead of temperature and salinity.
- advave, advct:
  1. Make diffusion terms agree with the basic Equations (7)–(10).
  2. Force diffusive and convective fluxes to be zero on land points.

REFERENCES

1. Werner FE. A field test case for tidally forced flows. A review of the tidal flow forum. In *Quantitative Skill Assessment for Coastal Ocean Models*, Lynch DR, Davies AM (eds). American Geophysical Union: Washington, DC, 1995.
2. Røed LP, Hackett B, Gjevik B, Eide LI. A review of the metocean modeling project (MOMOP), part 1: Model comparison study. In *Quantitative Skill Assessment for Coastal Ocean Models*, Lynch DR, Davies AM (eds). American Geophysical Union: Washington, DC, 1995.
3. Berntsen J, Svendsen E, Ostrowski M. *Validation and Sensitivity Study of a Sigma-Coordinate Ocean Model Using the Skagex Dataset*. International Council for the Exploration of the Sea, 1996 (CM 1996/C:5).
4. Gresho PM, Sani RL. Introducing four benchmark solutions. *International Journal for Numerical Methods in Fluids* 1990; **11**: 951–952.
5. Lynch DR, Davies AM (eds). *Quantitative Skill Assessment for Coastal Ocean Models. Coastal and Estuarine Studies*, vol. 47. American Geophysical Union: Washington, DC, 1995.
6. Haidvogel DB, Beckmann A. *Numerical Ocean Circulation Modelling*. Imperial College Press, 1999.
7. Blumberg AF, Mellor GL. A description of a three-dimensional coastal ocean circulation model. In *Three-Dimensional Coastal Ocean Models*, vol. 4, Heaps N (ed.). American Geophysical Union: Washington, DC, 1987.
8. Berntsen J, Skogen MD, Espelid TO. Description of a σ-coordinate ocean model, 1996. Technical Report Fisken og Havet Nr. 12, Institute of Marine Research.
9. Mesinger F, Arakawa A. *Numerical Methods Used in Atmospheric Models*, vol. I. Garp Publication Series No. 17, 1976.
10. Mellor GL, Blumberg AF. Modelling vertical and horizontal diffusivities in the sigma coordinate system. *Monthly Weather Review* 1985; **113**: 1379–1383.
11. Avlesen H, Berntsen J, Espelid TO. A convergence study of two prognostic, sigma coordinate ocean models on a density driven flow in a quadratic basin, 1998. Technical Report 157, Department of Informatics, University of Bergen, Norway, 1998.